

# Supplementary material to: “Radiation stability of nanocrystalline single phase multicomponent alloys”

E. Levo<sup>\*1</sup>, F. Granberg<sup>†1</sup>, D. Utt<sup>2</sup>, K. Albe<sup>2</sup>, K. Nordlund<sup>1</sup>, and F. Djurabekova<sup>3,1,4</sup>

<sup>1</sup>Department of Physics, P.O. Box 43, FIN-00014, University of Helsinki, Finland

<sup>2</sup>Fachgebiet Materialmodellierung, Institut für Materialwissenschaft, TU Darmstadt, Otto-Berndt-Str. 3, D-64287 Darmstadt, Germany

<sup>3</sup>Helsinki Institute of Physics, P.O. Box 43, FIN-00014, University of Helsinki, Finland

<sup>4</sup>National Research Nuclear University MEPhI, Kashirskoe avenue, 31 Moscow, Russia

## 1 Snapshots of the defect structures

Snapshots of the “Case 2” simulation cells in different materials and potentials can be found in Figs. 1, 2 and 3. The snapshots are taken after 500 cascades in the Zhou *et al.* potential, after 1500 cascades in the Bonny *et al.* potential and after 1000 cascades in the Purja Pun *et al.* potential. The description of the figures can be found in the main article.

## 2 Potential energy calculations

Potential energy calculations for the different elements in the nanocrystalline simulation cells 0 K were done, and compared to single crystalline cells of 500 000 atoms. The resulting energy distributions for the atoms can be seen in Figs. 4, 5 and 6. The plots are normalized so that the areas under the curves are equal to one.

## 3 Energy change during irradiation

The energy change of the system during irradiation can be found in Figs. 7, 8 and 9, for all three potentials. The energy shown in the graphs is the energy of the system at certain doses compared to the corresponding unirradiated system.

---

\*emil.levo@helsinki.fi

†fredric.granberg@helsinki.fi

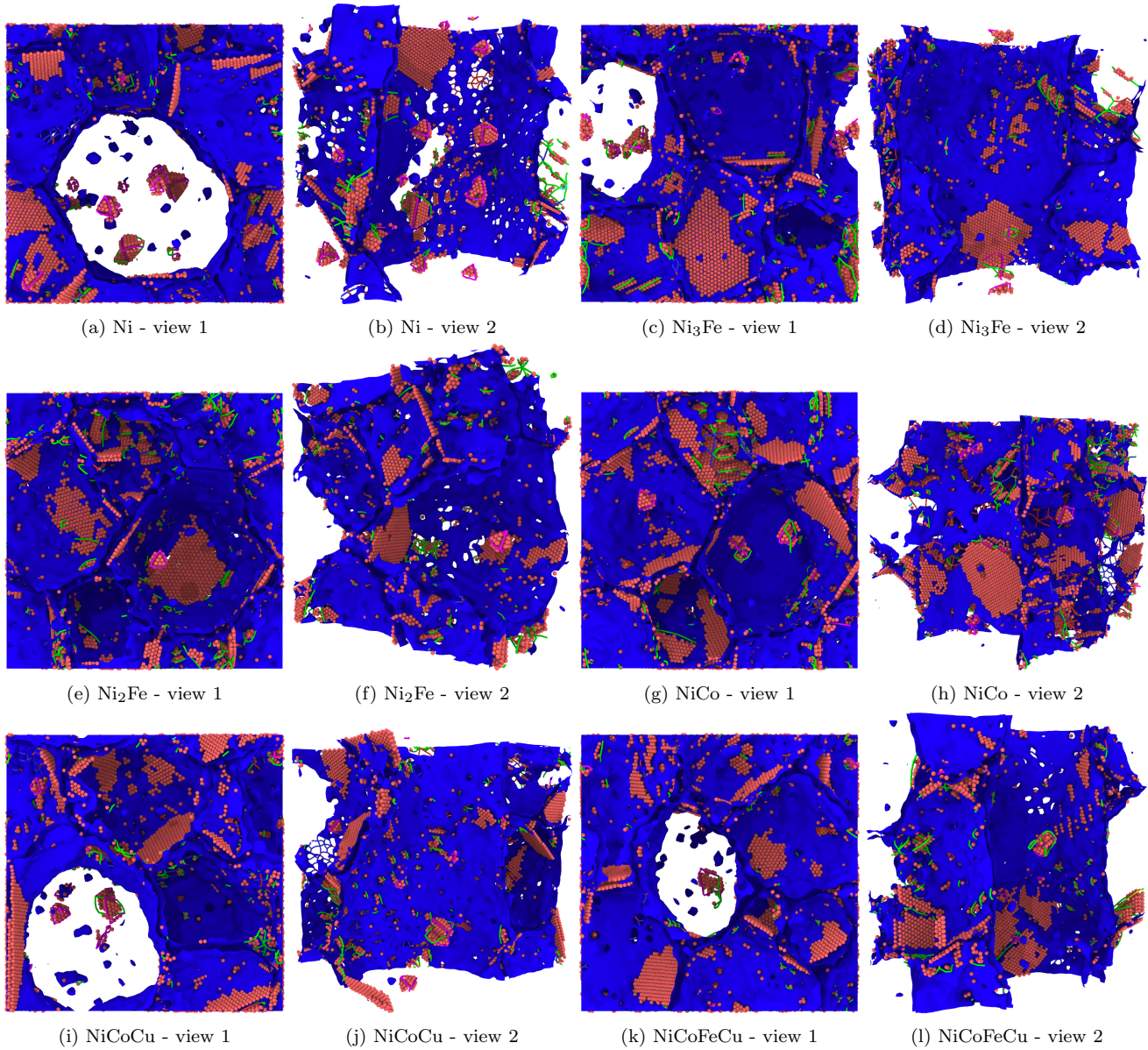


Figure 1: Snapshots of the defect structures in all materials for the Zhou *et al.* potential after the 500th cascade.

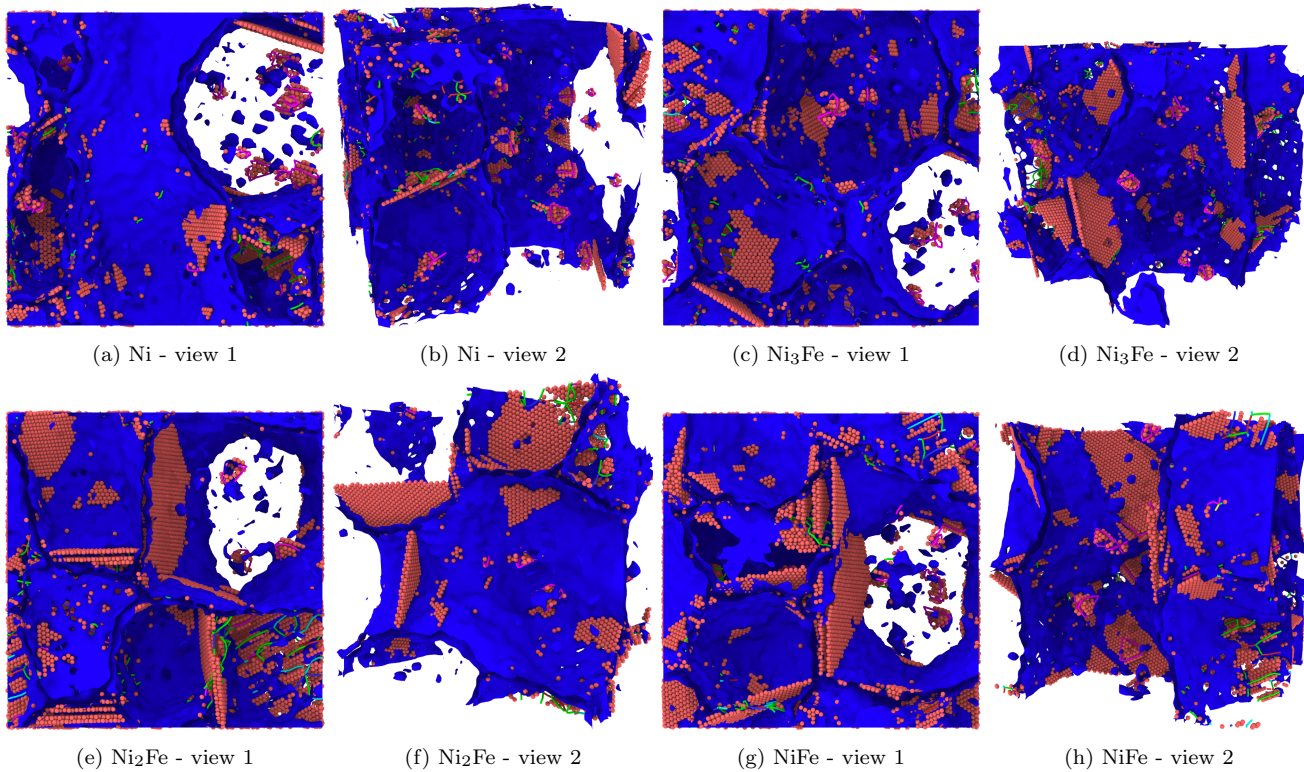


Figure 2: Snapshots of the defect structures in Ni,  $\text{Ni}_3\text{Fe}$ ,  $\text{Ni}_2\text{Fe}$  and NiFe for the Bonny *et al.* potential after the 1500th cascade.

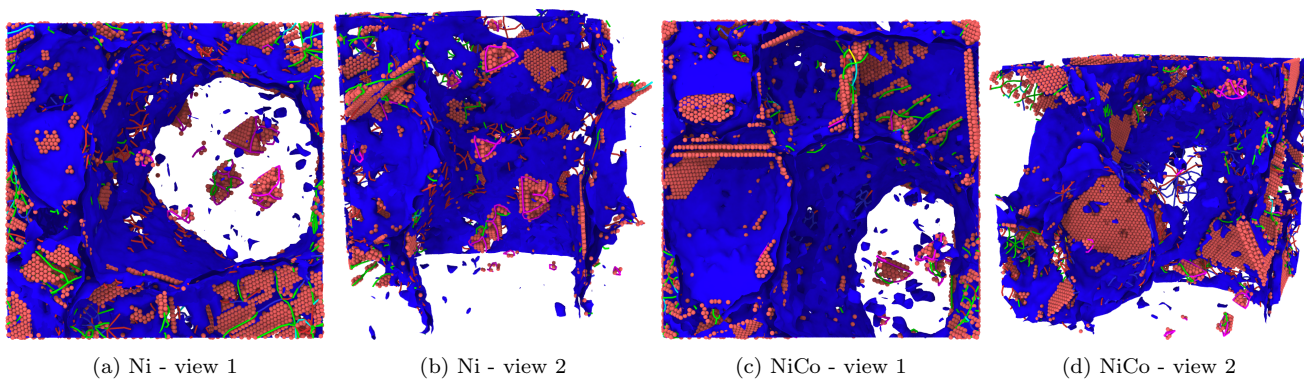


Figure 3: Snapshots of the defect structures in Ni and NiCo for the Purja Pun *et al.* potential after the 1000th cascade.

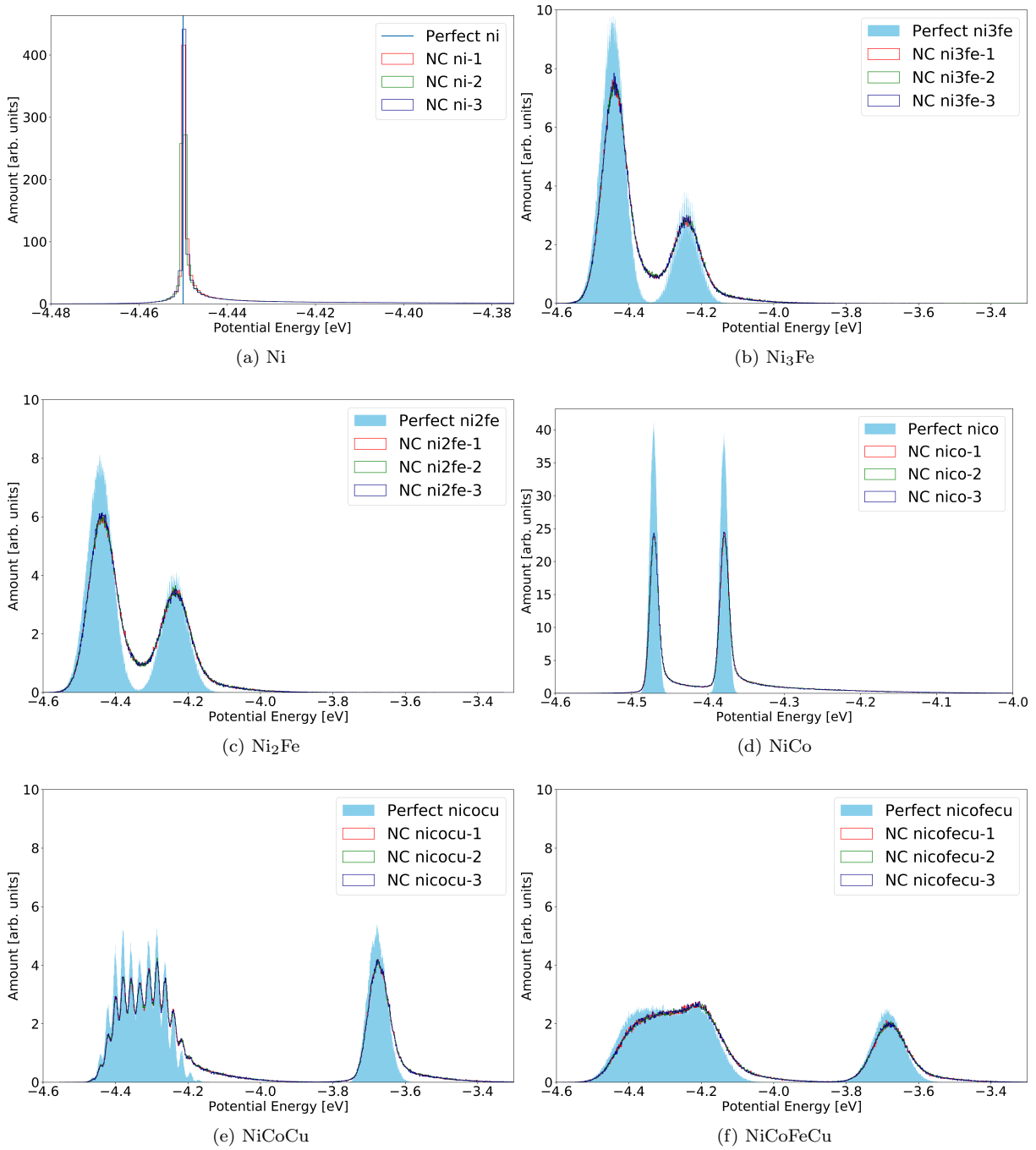


Figure 4: Energy distribution of all atoms in single and nanocrystalline cells relaxed to 0 K for the Zhou *et al.* potential. The shaded area is the single crystalline sample and the lines the different cases of the nanocrystalline samples. The plots have been normalized so that the area under the curve is equal to one.

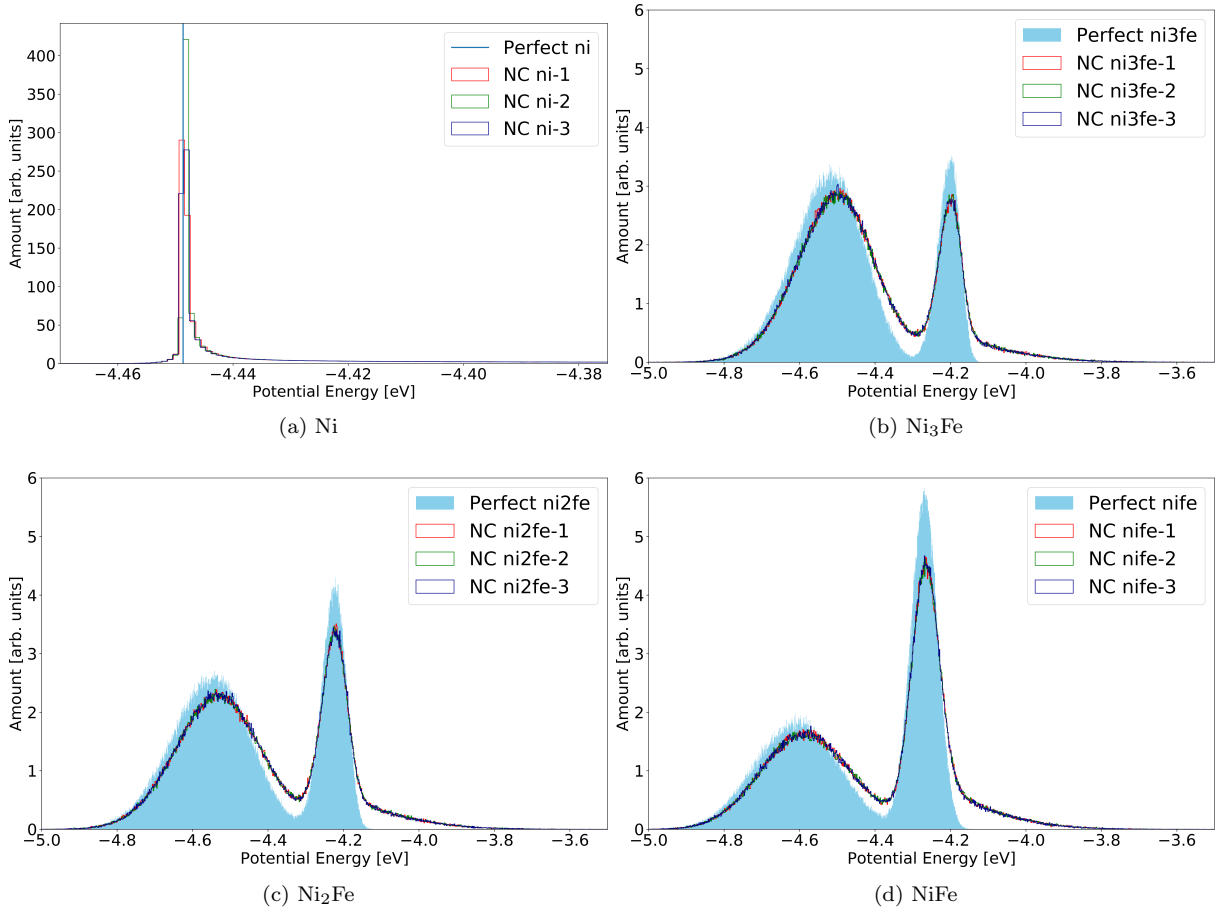


Figure 5: Energy distribution of all atoms in single and nanocrystalline cells relaxed to 0 K for the Bonny *et al.* potential. The shaded area is the single crystalline sample and the lines the different cases of the nanocrystalline samples. The plots have been normalized so that the area under the curve is equal to one.

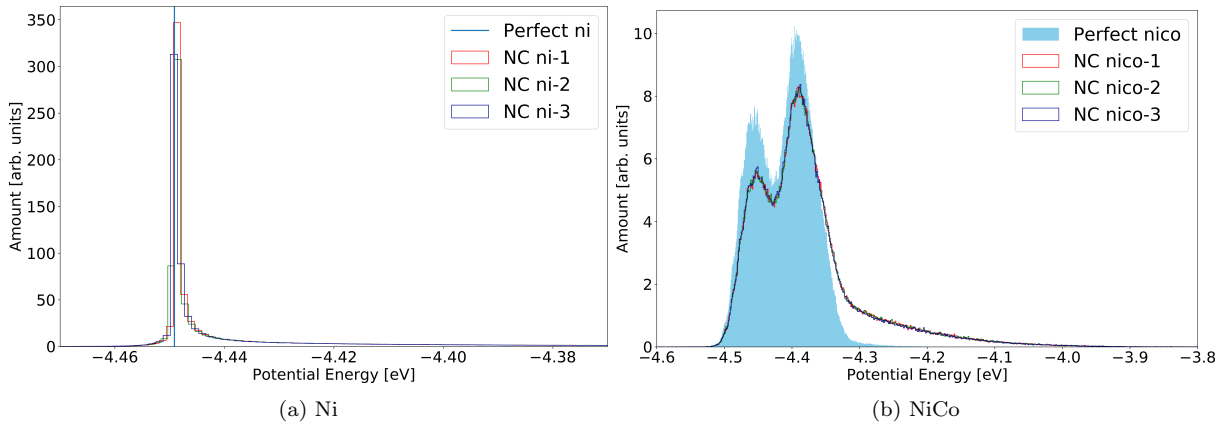


Figure 6: Energy distribution of all atoms in single and nanocrystalline cells relaxed to 0 K for the Purja Pun *et al.* potential. The shaded area is the single crystalline sample and the lines the different cases of the nanocrystalline samples. The plots have been normalized so that the area under the curve is equal to one.

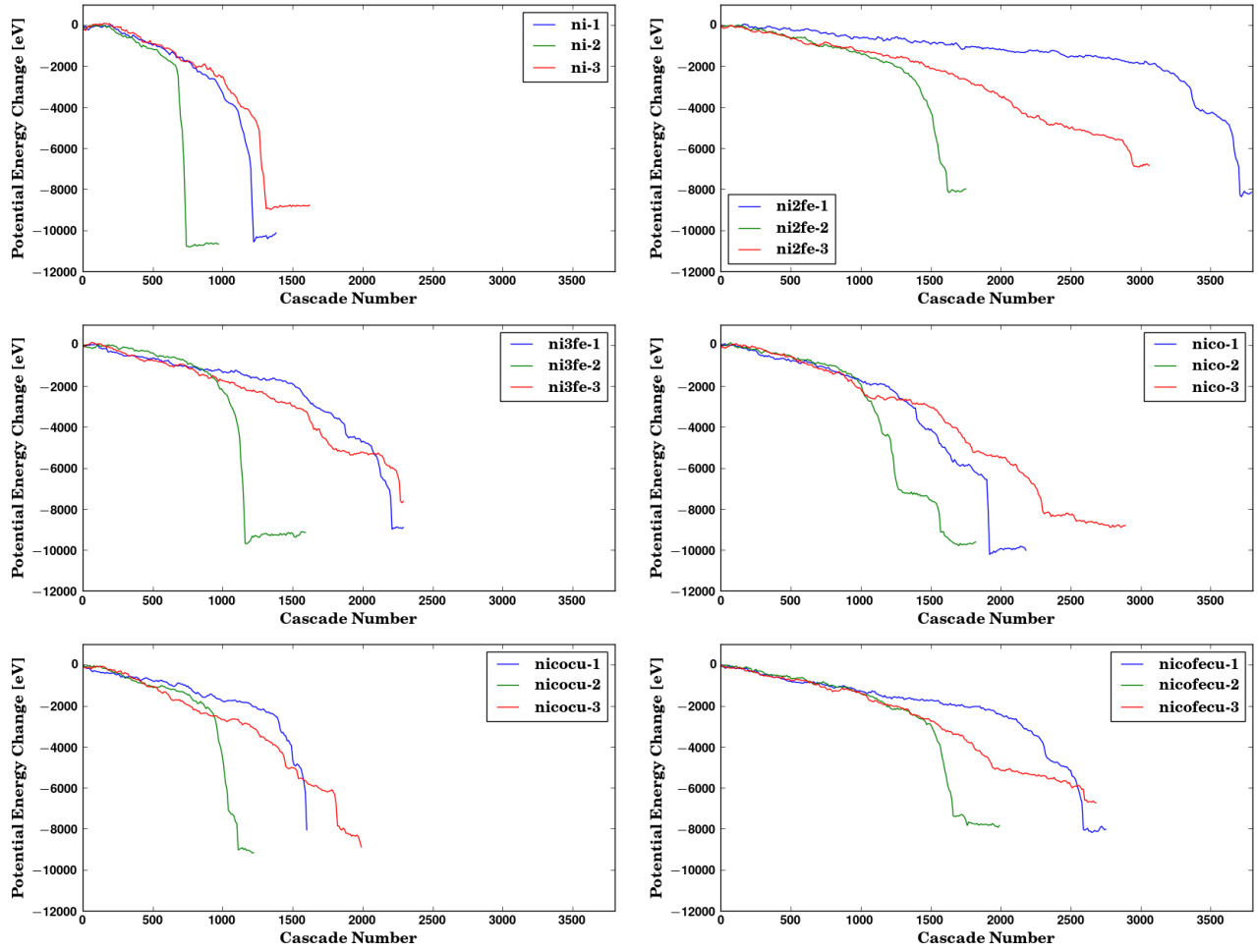


Figure 7: Potential energy change in the Zhou *et al.* potential.

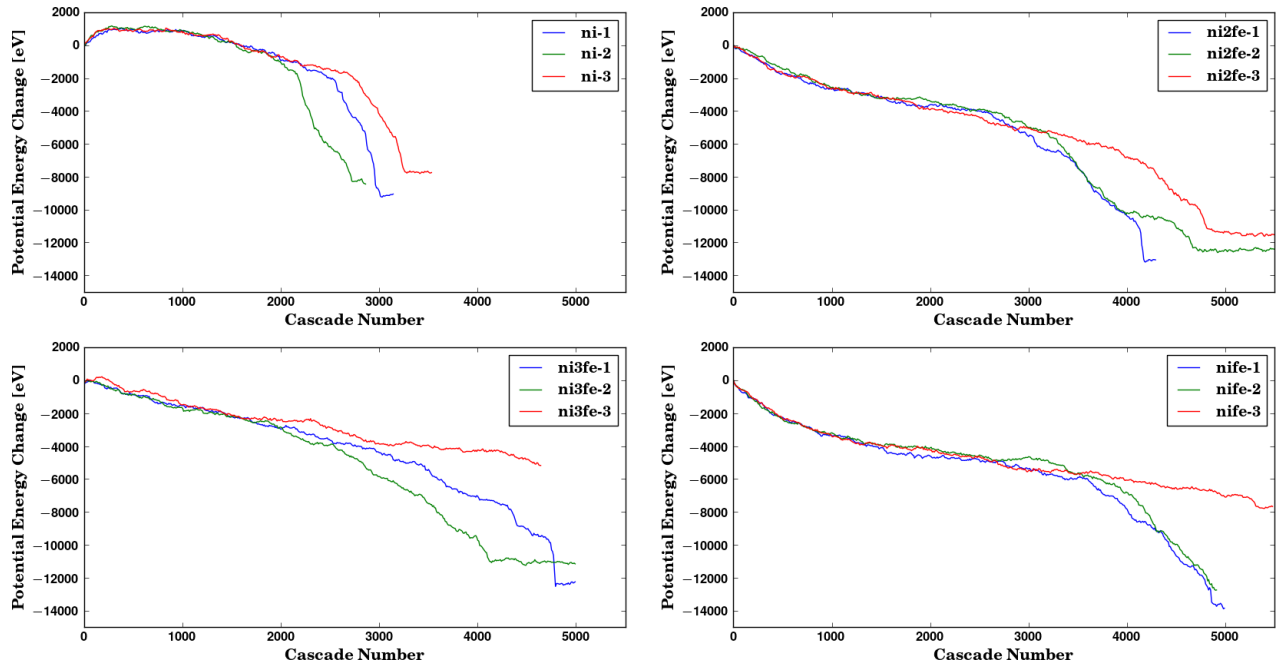


Figure 8: Potential energy change in the Bonny *et al.* potential.

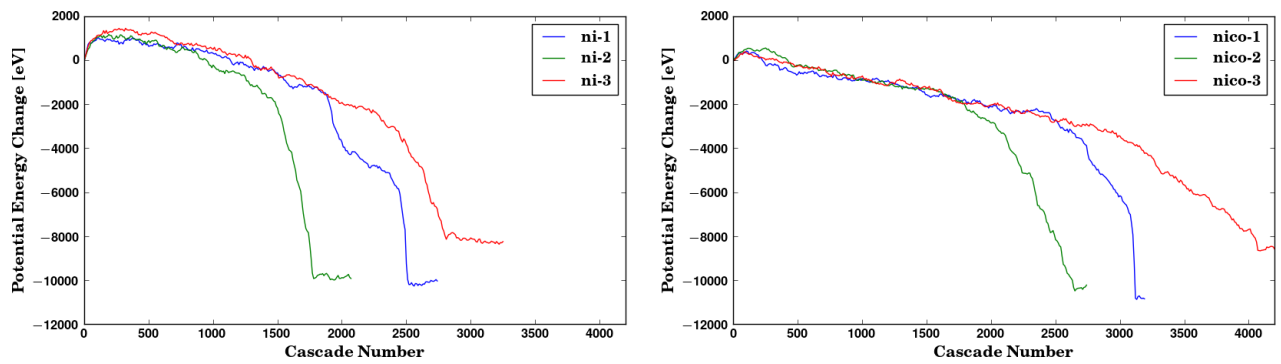


Figure 9: Potential energy change in the Purja Pun *et al.* potential.